This is an *Accepted Manuscript*, which has been through the Royal Society of Chemistry peer review process and has been accepted for publication.

Accepted Manuscripts are published online shortly after acceptance, before technical editing, formatting and proof reading. Using this free service, authors can make their results available to the community, in citable form, before we publish the edited article. We will replace this *Accepted Manuscript* with the edited and formatted *Advance Article* as soon as it is available.

You can find more information about *Accepted Manuscripts* in the **Information for Authors**.

Please note that technical editing may introduce minor changes to the text and/or graphics, which may alter content. The journal's standard **Terms & Conditions** and the **Ethical guidelines** still apply. In no event shall the Royal Society of Chemistry be held responsible for any errors or omissions in this *Accepted Manuscript* or any consequences arising from the use of any information it contains.

Organic & Biomolecular Chemistry

Paper

A Merocyanine-based Colorimetric and Ratiometric Fluorescent Probe for Specifically Distinguishing Cysteine from Biothiols in Water and Imaging Application in Living Cells

Qingxin Han,[a] Zhaohua Shi,[a] Xiaoliang Tang,[a] Lizi Yang,[a] Zuolin Mou,[a] Jing Li,[b] Jinmin Shi,[a] Chunyang Chen,[a] Wei Liu,[a] Huan Yang[a] and Weisheng Liu *[a]

A merocyanine-based highly selective colorimetric and ratiometric fluorescent probe was described for Cys detection in water and diluted deproteinized human serum. Upon reaction with Cys in aqueous buffer solution, the probe showed dramatic color change from faint yellow to pink and remarkable ratiometric fluorescence enhancements signals was also observed, which are ascribed to an intramolecular charge transfer (ICT) progress. This strategy was based on modulating the merocyanine π-electron system by conjugation and removal of the acrylate group to release chromophore group, resulting in specific colorimetry and fluorescence response. The probe has low cytotoxicity and good cell permeability. It is readily employed for assessing the change of Cys level intracellular.

Introduction

In recent years, particular effort has been focused on the chemosensing of sulfhydryl-containing amino acids and peptides. Cysteine (Cys), as one of the most abundant intracellular biothiols, is involved in protein synthesis and is essential for maintaining the appropriate redox status of proteins, cells, or organisms.[1] Moreover, cysteine is implicated in the detoxification of toxic metals (cadmium, mercury), metabolism of zinc and copper, as well as scavenging of free radicals.[2] Cys has been associated with neurotoxicity,[3] slowed growth rate, hair depigmentation, edema, lethargy, liver damage, muscle and fat loss, skin lesions, and weakness,[4] Given that the vital physiological role in biological systems, accurate detection of Cys has become quite desired. In addition, other intracellular biothiols such as homocysteine (Hcy) and glutathione (GSH) play different important biological roles from Cys which were associated with different diseases, so quantification and discrimination of them is of great importance.[5] Since small-molecule fluorescent probes can make use of selective, bioorthogonal chemistries to report on specific analytes in cells and in more complex biological specimens,[6] fluorimetry is acceptable for recognizing Cys.

To date, numerous fluorescent probes based on Michael additions,[7] cyclization reactions with aldehyde,[8] cleavage reaction[9] and others[10] have been developed for the detection of biothiols. However, most of them need ultraviolet excitation and only a few of them could significantly distinguish Cys from Hcy.[11] More importantly, those documented probe have certain limitation of aqueous solubility or couldn't be applied in 100% water. Reactivity in nucleophilic reactions is noteworthy to take into consideration for the SH group steric shielded in GSH molecular and the higher thiolate/thiol ratio for Cys at neutral pH than other biologically important thiols, including Hcy.[11e] Condensation of α, β-unsaturated ketone moiety with Cys to discriminate Cys and Hcy was reported by Strongin *et al.*[11b] and Yoon *et al.* .[11d] Nevertheless, both required organic solvents. Subsequently, a seminaphthofluorescein-based fluorescent probe for Cys in cetyltrimethylammonium bromide media buffer was reported,[12] however, it has not been used in biological application. Therefore, it occurred to us to design a fluorescent probe with properties of good aqueous solubility, high sensitivity, biocompatibility and quick response for real-time detection for Cys.

As an overall strategy, merocyanine dyes was chosen as our fluorophore by its strong intramolecular charge transfer (ICT) with "push–pull" substituent pairs.[13] Here, we present a simple merocyanine-based fluorescence probe **3,** in which an acrylate group is linked to fluorophore as the blockage of ICT process. Probe **3** could selectively detect Cys and exhibit a ratiometric fluorescence response in water and diluted deproteinized human serum. The hybrid density functional theory (DFT) calculation was performed to elucidate the electronic properties of this ICT system. Since Cys and Hcy have different relative rates of intramolecular cyclization,[14] the probe could specifically distinguish Cys over Hcy and GSH based on the kinetic profiles. In addition, fluorescence microscopy experiment has demonstrated that the probe is membrane permeable and can be exploited for bioimaging.

Experimental

General Information and Materials

All solvents were of reagent grade. (E)-2-(4-hydroxystyryl)-1,3,3-trimethyl-3H-indolium iodide (compound **2**) was synthesized according to the literature procedure.[15] The human plasma samples were deproteinized by using the procedure as described in the literature.[16] Oxygen-sensitive reaction was carried out under an argon atmosphere in heat-dried flask. All reactions were monitored by thin-layer chromatography (TLC) using UV light. ^{1}H NMR and ^{13}C NMR spectra were recorded on a Bruker DRX400 spectrometer and referenced to the solvent signals or tetramethylsilane. Mass spectra (ESI) were performed on a LQC system (Finngan MAT, USA). The 1,2,3,3-tetramethyl-3H-indolium iodide derivatives were unstable in high temperature that no melting points were provided. Elemental analyses were conducted using an Elemental Vario EL. All pH measurements were made with a pH-10C digital pH meter. The fluorescence images of cells were taken using a BX53 fluorescence microscope (Japan Olympus Co., Ltd) with an objective lens (× 40). Single-crystal X-ray diffraction measurements were carried out on a Bruker APEX-II CCD diffractometer operating at 50 KV and 30 mA using Mo Kα radiation ($\lambda = 0.71073$Å).

All UV-visible spectra and fluorescence spectra were recorded using a Varian Cary 100 spectrophotometer and a Hitachi F-7000 luminescence spectrometer, respectively. The path length was 1 cm with a cell volume of 3.0 mL. Fluorescence responses of **3** to various metal ions were measured as follows: **3** (final, 10 μM) was added to 1 mL of phosphate buffer (10 mM, pH 7.40), then aqueous solution of different amounts of amino acids (Ala, Arg, Asp, Cys, Gln, Glu, His, Ire, Gly, Asn, Leu, Lys, Met, Phe, Pro, Ser, Thr, Trp, Tyr(dissolved in DMSO), Val and Hcy), physiologically important metal ions (Na^+, K^+, Ca^{2+}, Mg^{2+}, Fe^{3+}, Zn^{2+}) and redox species (H_2O_2, H_2S and GSH) in distilled water were used to give a final concentration of 0.1 mM.

Product Analysis

For ESI-MS analysis, a 0.2 mM solution of Cys in distilled water was added to a 10 μM probe **3** solution in EtOH. The mixtures were kept room temperature for 10 min and measured directly using ESI-TOF. For HPLC analysis, the above samples were analyzed with a reverse phase HPLC (Varian-ProStar system, 4.6 × 250 mm,

Diamonsil@C[18] 5μ) eluted with CH_3CN/H_2O. The retention time was compared with that of an authentic sample (E)-2-(4-hydroxystyryl)-1,3,3-trimethyl-3H-indolium iodide. For ^{1}H NMR analysis, to a solution of **3** (15 mg) in D_2O/CD_3OD (1:1), add 1 eq of Cys and then kept for 0.5 h before recorded on a Bruker DRX400 spectrometer.

Cell Culture and Fluorescence Microscopic Imaging

The *Hela* cell lines were provided by the Institute of Biochemistry and Cell Biology (China). Cells were grown in Dulbecco's modified eagle's medium (DMEM) supplemented with 10% fetal bovine serum in an atmosphere of 5% CO_2 and 95% air at 37 °C humidified air for 24 h. One day before imaging, the cells were passaged and plated in phenol red-free medium on 14 mm glass coverslips in 12-well plates. The solution of probe **3** in H_2O was diluted into DMEM, added to the cells and incubated for 0.5 hours. For the control experiment, cells were pretreated with 100 μM N-ethylmaleimide for 1.0 h, and then incubated with 50 μM probe **3** for 0.5 h at 37 °C. Before analysis, the coverslips were removed from the 12-well plate and plated on a glass slide. Then fluorescence microscopic images were acquired at blue channel. The microscope settings (brightness, contrast, and exposure time) were held constant before and after pretreatment of cells with N-ethylmaleimide to compare the relative intensity of intracellular cysteine fluorescence.

Determination of cell viability Cell viability was determined by MTT assays. *HeLa* cells (1×10^4 cells/well) were placed in a flat-bottom 96-well plate in 100 μL culture medium and incubated in 5% CO_2 at 37 °C. After overnight incubation, the cells were treated with various concentrations (0, 5, 10, 25, 50 μM) of probe **3** and compound **2**. After incubating the cells with probe **3** or compound **2** for 24 h, the MTT reagent (5 mg/mL) was then added to each well (10 μL/well, 0.5 mg/mL) and incubated 4 h. The water-insoluble formazan crystal was dissolved by the addition of 100 μL of DMSO to each well. The optical density of each well was measured with a Perkin Elmer VICTOR3 1420 Multilabel Plate Reader at 570 nm. The relative cell viability (mean% ± SD, n = 3) was expressed as Abs compound/Abs control, where Abs control was obtained in the absence of the compounds.

Kinetic Studies

The reaction of probe **3** (5.0×10^{-6} M) with Cys, Hcy and GSH in phosphate buffer (10 mM, pH 7.40) at room temperature was monitored by measuring the fluorescence intensity ratio R (I_{552}/I_{502}). The apparent rate constant for the reaction was determined by fitting the fluorescence intensity ratios of the samples to the pseudo first-order equation:

$$Ln((R_{max} - R_t)/R_{max}) = - k' t \tag{1}$$

Where R_t and R_{max} are the ratio of fluorescent intensities at 552 to that at 502 nm at times t and the maximum value obtained after the reaction was complete. K' is the apparent rate constant. The first-order rate constant k ($M^{-1} s^{-1}$), was obtained from Equation (2),

$$k' = k[M] \tag{2}$$

Where [M] is the concentration of Cys, Hcy and GSH.

Results and discussion

Reaction with Cys and Stability

It is well known that probe functioning through ICT undergoes a spectral shift, the ICT efficiency of the probe should be modulated upon interaction with specific analyte. The Cys-mediated removal of the electron-withdrawing acrylate group releases a hydroxy donor, increasing the "push-pull" character of the dye and resulting in alteration in the absorption and emission spectra. The synthesis of probe **3** and proposed reaction sequence is outlined in Scheme 1. Cys can react with the acrylate group to yield an intermediate thioethers involved the conjugate addition, which can further generate the compound **2** (enol form) and **4** via an intramolecular cyclization reaction.[11b] The deprotonation of hydroxy merocyanine **2** (enol form) results in the generation of keto form at neutral condition. As shown in Fig. 1, enol form has maximum absorption and fluorescence peaks at 425 nm and 510 nm, respectively. While the phenolate form shows an absorption band around 512 nm and emission peak at 552 nm in aqueous solution. In the case of Hcy and GSH, the kinetic rate of the intramolecular adduct/cyclization reactions leads to different fluorescence responses[11b,11d]. One can observe the emission at 488 nm steadily increasing over time, with a subsequent decrease (Fig. S1). The detailed NMR spectra for the **3** and **3**-Cys adducts are depicted in Fig. 2. The signals of the acryloyl protons of **3** appear at 7.65, 7.75, and 6.99 ppm, respectively. Then, the ^{1}H NMR spectrum of **3** in a solution of D_2O/CD_3OD (1:1) was monitored upon the addition of Cys at room temperature. Comparison of the ^{1}H NMR spectrum of the reaction mixture with those of **3** and compound **2** (enol form) shows that the decrease of probe **3** protons is accompanied by signals formation in agreement with those of compound **2**. The ESI spectrometry analysis of probe **3** treated with Cys in aqueous solution (10 mM PBS buffer, pH 7.40) also confirms the formation of the **3**-Cys adduct and compound **2**. The mass spectrum displays two peaks at *m/z* 453.3 and 263.3, respectively. Meanwhile, HPLC analysis of the reaction mixture reveals that there is an anticipative production, compound **2** (Fig. S2).

As there is an ester group in probe **3**, we first tested the stability of our probe. As shown in Fig, 3, the absorbance ratio (A_{512}/A_{384}) of probe **3** only increased from 0.065 to 0.101 after 2 hours of incubation in PBS buffer (10 mM, pH 7.40, 20 μM Probe **3**). But the addition of 10 eq Cys led the absorbance ratios already increase to 4.075 at 10 min. This result suggests that probe **3** is very stable in phosphate buffer. For N-ethylmaleimide (NEM, a well-known thiol-blocking agent) pretreated diluted deproteinized human plasma as well as *Hela* cells (Fig.S3), the addition of probe **3** reached the same result.
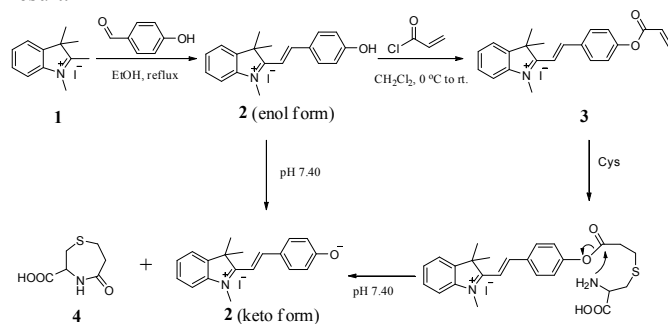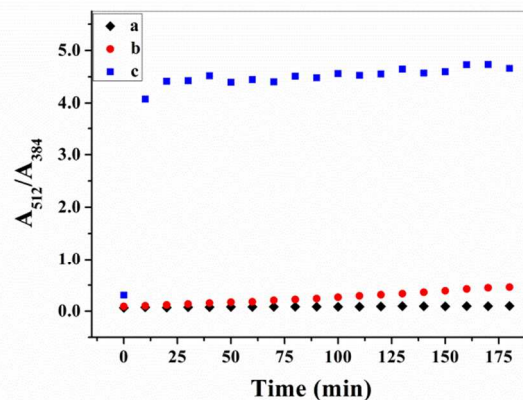

Scheme 1. Synthetic route for probe **3** and proposed reaction sequence with Cys.
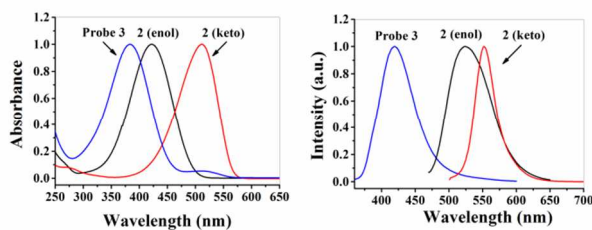
Fig. 1. Normalized absorption (left) and emission spectra (right) of probe 3 (λ_{ex} = 340 nm), compound **2** (enol form) (λ_{ex} = 418 nm, pH = 4.00), compound 2 (keto form) (λ_{ex} = 490 nm, pH = 8.00) in water.
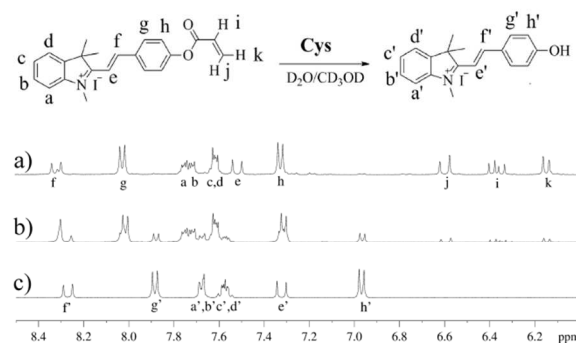
Fig. 2. Partial ^{1}H NMR spectra in D_2O/CD_3OD (1:1, *V/V*) at 25 $^{\circ}$C: **a**) Probe **3**; **b**) Probe **3** with Cys (1 equiv), 30 min; **c**) Compound **2**.

Fig. 3. Time-dependent absorbance ratio A_{512}/A_{384} of probe **3** (20 μM). **a**) Probe **3** in PBS buffer (10 mM, pH = 7.40) in the absence of Cys; **b**) Probe **3** in diluted deproteinized human plasma (0.2 mM N-methylmaleimide pretreated for 1h) in the absence of Cys; **c**) Probe **3** (20 in phosphate buffer (10 mM, pH = 7.40) in the presence of Cys (10 equiv).

Effect of pH and kinetic analysis To verify whether the probe is suitable for the physiological detection, we evaluated the effect of pH on the fluorescence of the probe **3**. As shown in Fig. S4, the probe and compound **2** were stable within the pH range of 6.0-9.0,

which indicates that the probe **3** possesses high sensing ability without interference from pH effects. Subsequently, based on the time-dependent fluorescence spectra, the reaction kinetic rates of probe **3** with Cys, Hcy and GSH were also examined (Fig. S5). The reaction for Cys was fast and the pseudo-first-order rate constant was 0.192 min^{-1}, while that for Hcy and GSH were only 0.031 min^{-1}, 0.006 min^{-1}, respectively. These data clearly confirmed that the probe could specifically detect cysteine over homocysteine and glutathione in the kinetic profiles.

Absorbance and fluorescence spectra study

The absorption and fluorescence spectra of the probe were examined under simulated physiological conditions (10 mM PBS, pH 7.40, 10 μM Probe **3**). The absorption spectra of probe **3** shows an absorption band at 384 nm (Fig. 4(a)). Upon addition of Cys (0.1 mM), the band centered at 384 nm shows apparent decrease in absorbance along with the appearance of a new absorption band at 512 nm, which is visible to the naked eye with a clear color change from pale yellow to pink. The variation in the absorption spectrum of probe **3** after treated with Cys led to the formation of a clear isosbestic point at 418 nm. We attributed the shift in lambda max to the change in structure. Moreover, the time-dependent changes in the absorption spectra (Fig. S6) and the absorption titration of probe **3** with Cys (Fig. 4(b)) further indicated that compound **3** could serve as a "naked-eye" probe for Cys. As shown in Fig. S7, probe **3** also displayed excellent color selectivity for Cys.

Apart from the results obtained from UV−*vis* studies, fluorometric detection of Cys with probe at different excitation wavelengths was also evaluated. When excited at 418 nm, the fluorescence of probe **3** undergoes a significant red shift from λ max 488 nm to λ max 552 nm with an isoemissive point at 502 nm upon the addition of Cys (Fig. 5). This properties illustrating that the chemical transformation from acrylate group to hydroxyl group modulated the ICT efficiency of the fluorophore, and thereby resulted in ratiometric changes in both color and fluorescence. In short, the addition of Cys modulated the "push-pull" character of the dye by removal of the acrylate group, lead to a better donor acceptor system and changed the fluorescence emission of merocyanine.
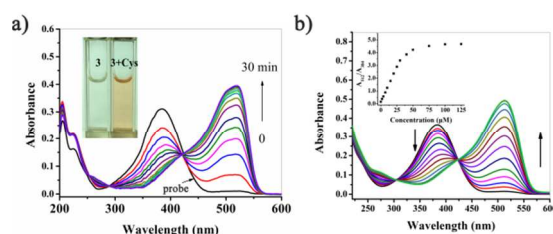
Fig. 4. a) Time-dependent UV-vis spectral changes of probe **3** (10 μM) with Cys (10 equiv) in phosphate buffer (10 mM, pH 7.40). Inset: The color change of probe **3** in phosphate buffer (10 mM, pH = 7.40) without and with addition of Cys. **b)** Absorption spectra of probe **3** (10 μM) with the titration of Cys (1, 2, 4, 7, 10, 15, 20, 35, 50, 75, 100, 125, and 150 μM) in phosphate buffer (10 mM, pH 7.4).

Inset: Absorbance ratio (A_{512}/A_{384}) change of probe **3** at 10 min as a function of concentration Cys.
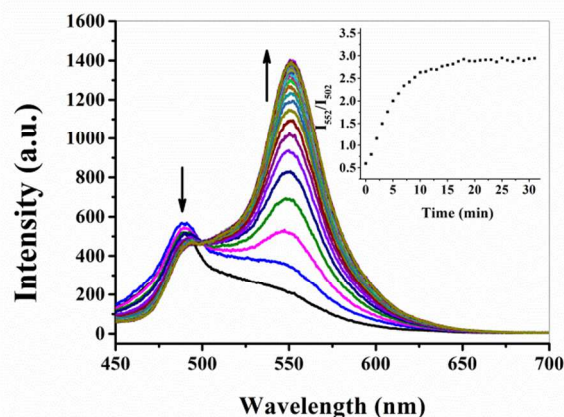
Fig. 5. Time-dependent fluorescence spectral changes of probe **3** (10 μM) with Cys (10 equiv) in phosphate buffer (10 mM, pH 7.40). λ_{ex} = 418 nm. Inset: Fluorescence intensity ratio R (I_{552}/I_{502}) *vs* time.

Sensitivity and selectivity to Cys

High selectivity toward Cys in the presence of other competitive species is a very important feature to evaluate the performance of the fluorescent probe **3**. Therefore, selectivity and competition experiments were also conducted in aqueous solution (10 mM PBS, pH 7.40). As shown in Fig. S8, upon excitation at the isosbestic point at 418 nm in the presence of different concentrations of Cys, however, a unique ratiometric fluorescent change was observed for probe **3**. These changes in the fluorescence spectrum stopped when the amount of added Cys reached to 75μM. At this amount fluorescence intensity ratios R (I_{512}/I_{502}) became as high as 5 times that in the absence of Cys. Interestingly, the fluorescence intensity increased linearly when the Cys concentration increased from 0 to 40 μM. The detection limit (LOD) was measured to be 0.5 μM. Addition of other amino acid and biological thiols did not lead to any fluorescence intensity fluctuation except that Hcy and GSH showed slightly enhanced fluorescence during the test time. However, Hcy and GSH could not induce obvious fluorescence enhancement if the reaction time was shortened (Fig. S9).Furthermore, important metal ions, other amino acid and redox species, such as Na^{+}, K^{+}, Ca^{2+}, Mg^{2+}, Fe^{3+}, Zn^{2+}, H_2O_2 and H_2S, had little interference in the sensing properties of probe **3** (Fig. 6). The response of probe **3** to Cys in the presence of other competing amino acid was demonstrated in PBS buffer (10 mM, pH 7.40) to further assess the selectivity of the probe for Cys (Fig. 7). The fluorescence intensity was hardly interfered by other coexistent amino acid. The above results suggested that probe **3** was a highly selective fluorescent probe for Cys in aqueous solution.
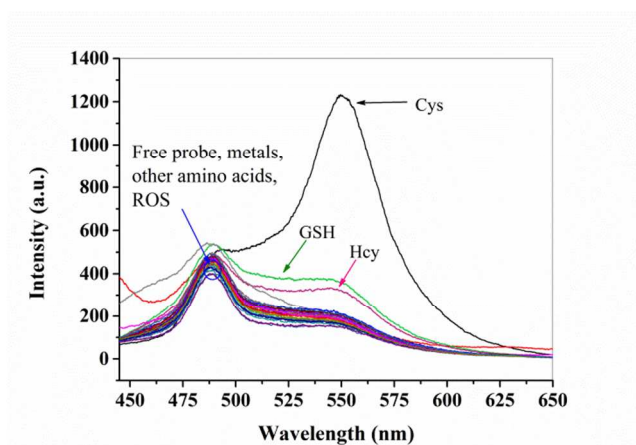
Fig. 6. Fluorescence responses of probe **3** with 100 μM various analytes (Cys, Hcy, GSH, Ala, Aln, Arg, Asp, Gln, Glu, Gly, His, Ire, Leu, Lys, Met, Phe, Pro, Ser, Thr, Trp, Tyr, Val, Na$^+$, K$^+$, Ca^{2+}, Mg^{2+}, Fe^{3+}, Zn^{2+}, H$_2$O$_2$ and H$_2$S) in phosphate buffer (10 mM, pH 7.40), each spectrum was recorded at 10 min after the addition to probe **3**. λ_{ex} = 418 nm.
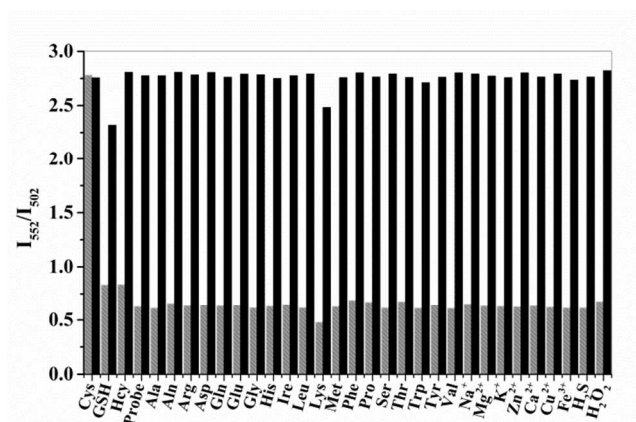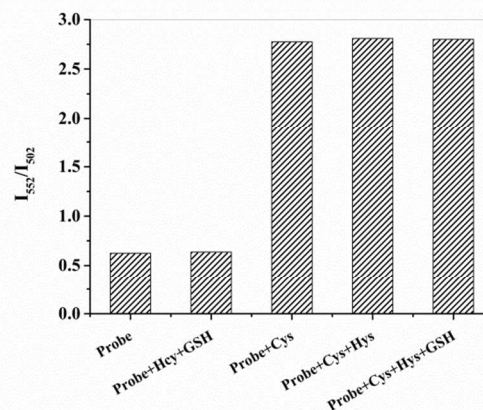

Fig. 7. Fluorescence intensity ratio R (I$_{552}$/I$_{502}$) of probe **3** (10 μM) in the presence of various analytes (100 μM) (Cys, Hcy, GSH, Ala, Aln, Arg, Asp, Gln, Glu, Gly, His, Ire, Leu, Lys, Met, Phe, Pro, Ser, Thr, Trp, Tyr, Val, Na$^+$, K$^+$, Ca^{2+}, Mg^{2+}, Fe^{3+}, Zn^{2+}, H$_2$O$_2$ and H$_2$S) in phosphate buffer (10 mM, pH 7.40) at 10 min, λ_{ex}=418 nm. Grey bars represent the addition of 10 equiv of the appropriate amino acids to a 10 μM solution of probe **3**. Black bars represent the addition of probe **3** (10 μM) to the mixture solution of 100 μM the appropriate amino acids and 100 μM Cys.

Detection of Cys in diluted deproteinized human plasma

In particular, lipid-water partition coefficient of the probe has been measured to be -0.22 (logP) in Octanol/Water. This result was consistent with the good water solubility. In addition, we explored the ability of the probe to detect Cys in diluted (30%) deproteinized human plasma. Total Hcy and GSH concentration in healthy human plasma is approximately 5–12 μM,[17] and 0.5 μM,[18] respectively. Cys concentration is approximately 20–30 times more that of Hcy.[19] A mixture of 30 μM Cys, 0.5 μM GSH, and 10 μM Hcy was used to

study possible effect of Hcy and GSH at physiological levels on the detection of Cys. As shown in Fig. 8, Hcy and GSH also exhibit little significant interference with the Cys assay at Hcy and GSH levels which are found to be proportional to those of Cys in plasma. Upon excitation at 418 nm, however, only a slightly fluorescence intensity ratio R (I$_{552}$/I$_{502}$) enhancement was observed as a result of the interference of strong background fluorescence in diluted deproteinized human plasma (Fig. S10a). When excited at 490 nm (Fig. S10b), the interference of background fluorescence is diminished and the emission intensity at 552 nm increased upon the gradual addition of Cys. Therefore, emission spectra upon excitation at 490 nm were studied (Fig. S11). The time course of the fluorescence assay showed that the fluorescence of the reaction with Cys is increasing with time and reaches a plateau at 10 min in aqueous solution. And furthermore, the linear calibration curves between fluorescence emission intensity/intensity ratio and Cys concentration in diluted deproteinized human plasma has been obtained (Fig. S12). Above results showed the potential utility of probe **3** in clinical diagnosis.
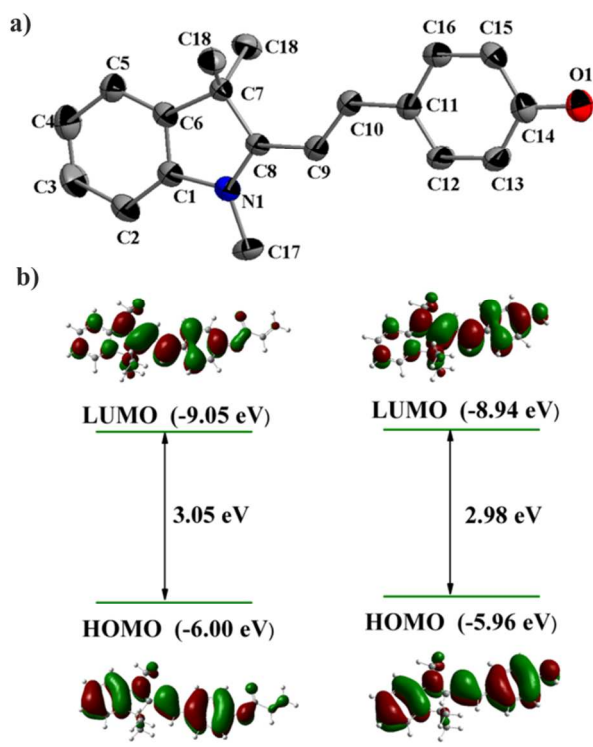

Fig. 8. Fluorescence intensity ratio R (I$_{552}$/I$_{502}$) (λ_{ex} = 418 nm) of probe (10 μM) in phosphate buffer (20 mM, pH 7.40) in the presence of mixtures of biothiols at 10 min. A concentration of Cys (30 μM) is present in the mixture of 0.5 μM GSH and Hcy (10.0 μM) to study Hcy and GSH and its possible effect at physiological levels on the detection of Cys.

Crystal structure and computational studies

Crystal of compound **2** (enol) was obtained by slow evaporation of the solvent from the MeOH solution. The molecular structure was shown in Fig. 9a. The compound **2** (enol) crystallizes in the orthorhombic space group *Pnma* and each molecule is found in the phenolic form. The bond length of C(14)–O(1) is 1.350(6) Å and this of C(10)–C(11) is 1.442(6) Å, which indicate single bonds, whereas a double bond is revealed from C(9)–C(10) being 1.349(6) Å. Furthermore, the bond angles C(7)–C(8)=C(9) and C(9)=C(10)–C(11) are 126.4(4)–126.1(4)°, indicating the sp^2-hybridization of the C(8) and C(9) atoms. Molecule of compound **2** (enol) is found completely planar with dihedral angles Φ between aromatic rings of 0.0°.

We used hybrid density functional theory (DFT) calculations to elucidate the mechanism of spectrum changes that accompanies formation of the putative compound **2**. These were implemented using the 6-31G(d) basis sets and a suite of Gaussian 09 W programs. For our study, B3LYP density functional[20] were used and the LANL2DZ effective core potential was used for all of the atom.[21] As shown in Fig. 9b. The optimized structures of compound **2** (enol) were very close to its single crystal X-ray diffraction structures. The HOMO in both probe **3** and compound **2** (enol) resides mainly on the merocyanine moiety. However, these two species difference at the level of the HOMO/LUMO. The energies of HOMO and LUMO of compound **2** (enol) are much higher than those of probe **3**. More importantly, the increasing energy in the LUMO is more obvious than that of the HOMO. Such differentiation leads us to predict the recovery of the D-π-A feature of the fluorophore and a bathochromic shift character by Cys-mediated cleavage in absorption. We found that the π-electrons of HOMO and LUMO in compound **2** (enol) is more localized on the merocyanine chromophore core, which actually translated to the change in the emission.[7b] This concordance supports the proposed intramolecular charge transfer sensing mechanism for probe **3**.
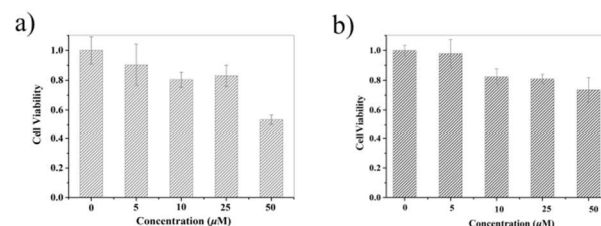
Due to the favorable properties of probe **3** *in vitro*, we established the ability of probe **3** for fluorescence imaging application by using a *Hela* cell model. *Hela* cell were incubated with probe **3** for 30 min in DMEM at 37 °C, the cells were washed with PBS buffer (10 mM, pH 7.40) to remove excess probe **3**, and then the cells were imaged by a fluorescence microscope. The cells treated with various concentrations of probe **3** displayed different fluorescence intensities (Fig. S13). The loaded cells displayed greenyellow fluorescence and the fluorescence grew brighter as the concentrations of probe **3** increased from 10 to 50 μM In contrast, in a control experiment, the cells were treated with N-ethylmaleimide (as a thiol blocking agent) and the probe sequencely, as a result we observed a remarkable fluorescence quenching (Fig. 10). For biological applications, the cytotoxicity in HeLa cells was determined by conventional MTT assays (Fig. 11). Upon exposure to concentrations of 0-50 μM probe **3** and its product compound **2** for 24 h, 54% and 73% of the *HeLa* cells remained viable respectively, indicating low toxicity under the experimental conditions. The result demonstrated that probe possess good membrane permeability and is suitable for imaging of Cys in living cells.
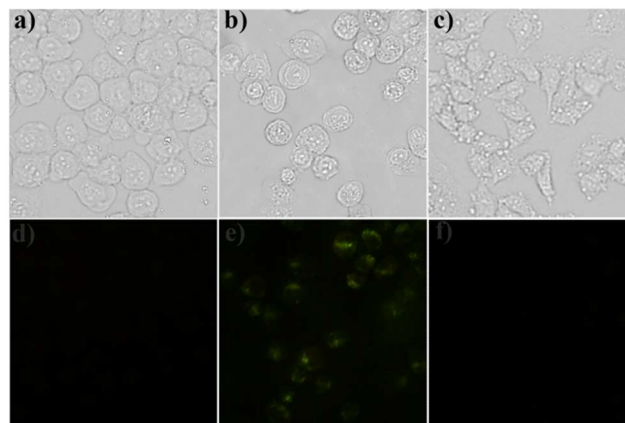
Fig. 10 Fluorescence images of Hela cells. **a)** Bright field images of cell. **b)** Bright field images of cells incubated with probe **3** (50 μM) for 30 min at 37 °C. **c)** Bright field images of cells pretreated with N-methylmaleimide (0.1 mM) for 30 min at 37 °C and then incubated with probe **3** (50 μM) for 30 min at 37 °C. **d)** Fluorescence images of cell. **e)** Fluorescence images of cells incubated with probe **3**. **f)** Fluorescence images of cells pretreated with N-methylmaleimide (0.1 mM) and probe **3**.

Fig. 9. a) Thermal ellipsoid (50% probability level) plot of compound **2** (enol form). All hydrogen atoms were deleted for clarity; **b)** Interfacial plots of the orbitals. (Left two): Probe **3** (LUMO and HOMO). (Right two): Compound **2** (LUMO and HOMO) calculated at B3LYP/6-31G(d) level. Green and reddish brown parts on the interfacial plots refer to the different phases of the molecular wave functions, for which the isovalue is 0.02 au.

Fluorescence microscopic images and cell viability

Fig. 11 MTT assay for the viability of HeLa treated with various concentrations of **a)** probe **3** and **b)**compound **2** for 24 h. Error bars represent the standard deviations of 3 trials.

Conclusions

In summary, we have developed a merocyanine-based probe **3** for discrimination of Cys from other structurally and functionally similar amino acids and thiols. It can also be used to sense Cys in water and diluted deproteinized human serum. Moreover, a colorimetric change makes the probe possible to detect Cys by the naked eye. The recognition of Cys should be attributed to modulate the "push-pull" character of the dye by conjugation and removal of the acrylate group. The limit of detection is 0.5 μM, which is sensitive enough for assessing Cys in biological systems. This probe has low cytotoxicity and good cell permeability, and can be applied for the imaging and biosensing of the Cys level changes in living cells. We anticipate that the fluorescent probe will be of great benefit for biomedical researchers to investigate the effects of Cys in biological systems.

Acknowledgements

Notes and references

[a] Key Laboratory of Nonferrous Metals Chemistry and Resources Utilization of Gansu Province and State Key Laboratory of Applied Organic Chemistry, Lanzhou University，Lanzhou University, Lanzhou 730000 (P. R. China)
Fax: (+86) 931 8912582
E-mail: liuws@lzu.edu.cn
[b] College of Pharmacy, Lanzhou University, Lanzhou 730000 (P. R. China)

† Electronic Supplementary Information (ESI) available. CCDC 970856. For ESI and crystallographic data in CIF or other electronic format see DOI: 10.1039/b000000x/

1.   (a) Z. A. Wood, E. Schröder, J. Robin Harris and L. B. Poole, *Trends Biochem. Sci,* 2003, **28**, 32-40; (b) J. B. Schulz, J. Lindenau, J. Seyfried and J. Dichgans, *Eur. J. Biochem.,* 2000, **267**, 4904-4911.

2.   T. Wlostowski, *BioMetals,* 1993, **6**, 71-76.

3.   X. F. Wang and M. S. Cynader, *J. Neurosci.,* 2001, **21**, 3322-3331.

4.   (a) S. Shahrokhian, *Anal. Chem.,* 2001, **73**, 5972-5978; (b) E. Weerapana, C. Wang, G. M. Simon, F. Richter, S. Khare, M. B. Dillon, D. A. Bachovchin, K. Mowen, D. Baker and B. F. Cravatt, *Nature,* 2010, **468**, 790-795.

5.   (a) L. L. Gluud, G. Dam, M. Borre, I. Les, J. Cordoba, G. Marchesini, N. K. Aagaard and H. Vilstrup, *Metab. Brain Dis.,* 2013, **28**, 221-225; (b) D. M. Townsend, K. D. Tew and H. Tapiero, *Biomed. Pharmacother.,* 2003, **57**, 145-155; (c) K. G. Reddie and K. S. Carroll, *Curr. Opin. Chem. Biol.,* 2008, **12**, 746-754.

6.   J. Chan, S. C. Dodani and C. J. Chang, *Nat. Chem.,* 2012, **4**, 973-984.

7.   (a) H. S. Jung, K. C. Ko, G. H. Kim, A. R. Lee, Y. C. Na, C. Kang, J. Y. Lee and J. S. Kim, *Org. Lett.,* 2011, **13**, 1498-1501; (b) L. Deng, W. Wu, H. Guo, J. Zhao, S. Ji, X. Zhang, X. Yuan and C. Zhang, *J. Org. Chem.,* 2011, **76**, 9294-9304; (c) B. K. McMahon and T. Gunnlaugsson, *J. Am. Chem. Soc.,* 2012, **134**, 10725-10728; (d) V. Hong, A. A. Kislukhin and M. G. Finn, *J. Am. Chem. Soc.,* 2009, **131**, 9986-9994; (e) H. S. Hewage and E. V. Anslyn, *J. Am. Chem. Soc.,* 2009, **131**, 13099-13106; (f) W. Lin, L. Yuan, Z. Cao, Y. Feng and L. Long, *Chem. Eur. J.,* 2009, **15**, 5096-5103; (g) H. Kwon, K. Lee and H. J. Kim, *Chem. Commun.,* 2011, **47**, 1773-1775; (h) X. Chen, S. K. Ko, M. J. Kim, I. Shin and J. Yoon, *Chem. Commun.,* 2010, **46**, 2751-2753; (i) L. Yi, H. Li, L. Sun, L. Liu, C. Zhang and Z. Xi, *Angew. Chem. Int. Ed.,* 2009, **48**, 4034-4037; (j) S. Sreejith, K. P. Divya and A. Ajayaghosh, *Angew. Chem. Int. Ed.,* 2008, **47**, 7883-7887; (k) X. Chen, S.-K. Ko, M. J. Kim, I. Shin and J. Yoon, *Chem. Commun.,* 2010, **46**, 2751-2753.

8.   (a) X. Zhang, X. Ren, Q. H. Xu, K. P. Loh and Z. K. Chen, *Org. Lett.,* 2009, **11**, 1257-1260; (b) W. Lin, L. Long, L. Yuan, Z. Cao, B. Chen and W. Tan, *Org. Lett.,* 2008, **10**, 5577-5580; (c) L. Xiong, Q. Zhao, H. Chen, Y. Wu, Z. Dong, Z. Zhou and F. Li, *Inorg. Chem.,* 2010, **49**, 6402-6408; (d) K. S. Lee, T. K. Kim, J. H. Lee, H. J. Kim and J. I. Hong, *Chem. Commun.,* 2008, 6173-6175.

9.   (a) M. M. Pires and J. Chmielewski, *Org. Lett.,* 2008, **10**, 837-840; (b) J. Bouffard, Y. Kim, T. M. Swager, R. Weissleder and S. A. Hilderbrand, *Org. Lett.,* 2008, **10**, 37-40; (c) X. Li, S. Qian, Q. He, B. Yang, J. Li and Y. Hu, *Org. Biomol. Chem.,* 2010, **8**, 3627-3630; (d) S. Ji, J. Yang, Q. Yang, S. Liu, M. Chen and J. Zhao, *J. Org. Chem.,* 2009, **74**, 4855-4865; (e) X. Cao, W. Lin and Q. Yu, *J. Org. Chem.,* 2011, **76**, 7423-7430; (f) B. Tang, Y. Xing, P. Li, N. Zhang, F. Yu and G. Yang, *J. Am. Chem. Soc.,* 2007, **129**, 11666-11667; (g) C. S. Lim, G. Masanta, H. J. Kim, J. H. Han, H. M. Kim and B. R. Cho, *J. Am. Chem. Soc.,* 2011, **133**, 11132-11135; (h) M. H. Lee, J. H. Han, P. S. Kwon, S. Bhuniya, J. Y. Kim, J. L. Sessler, C. Kang and J. S. Kim, *J. Am. Chem. Soc.,* 2012, **134**, 1316-1322; (i) J. H. Lee, C. S. Lim, Y. S. Tian, J. H. Han and B. R. Cho, *J. Am. Chem. Soc.,* 2010, **132**, 1216-1217; (j) J. Shao, H. Sun, H. Guo, S. Ji, J. Zhao, W. Wu, X. Yuan, C. Zhang and T. D. James, *Chem. Sci.,* 2012, **3**, 1049; (k) B. Zhu, X. Zhang, Y. Li, P. Wang, H. Zhang and X. Zhuang, *Chem. Commun.,* 2010, **46**, 5710-5712; (l) L. Long, W. Lin, B. Chen, W. Gao and L. Yuan, *Chem. Commun.,* 2011, **47**, 893-895.

10. (a) M. Zhang, M. Yu, F. Li, M. Zhu, M. Li, Y. Gao, L. Li, Z. Liu, J. Zhang, D. Zhang, T. Yi and C. Huang, *J. Am. Chem. Soc.,* 2007, **129**, 10322-10323; (b) Y. H. Ahn, J. S. Lee and Y. T. Chang, *J. Am. Chem. Soc.,* 2007, **129**, 4510-4511; (c) H. Y. Shiu, H. C. Chong, Y. C. Leung, M. K. Wong and C. M. Che, *Chem. Eur. J.,* 2010, **16**, 3308-3313; (d) Y. K. Yang, S. Shim and J. Tae, *Chem. Commun.,* 2010, **46**, 7766-7768; (e) H. S. Jung, J. H. Han, Y. Habata, C. Kang and J. S. Kim, *Chem. Commun.,* 2011, **47**, 5142-5144; (f) J. Shi, Y. Wang, X. Tang, W. Liu, H. Jiang, W. Dou and W. Liu, *Dyes Pigm.,* 2014, **100**, 255-260.

11. (a) H. Li, J. Fan, J. Wang, M. Tian, J. Du, S. Sun, P. Sun and X. Peng, *Chem. Commun.,* 2009, 5904-5906; (b) X. Yang, Y. Guo and R. M. Strongin, *Angew. Chem. Int. Ed.,* 2011, **50**, 10690-10693; (c) L. Yuan, W. Lin and Y. Yang, *Chem. Commun.,* 2011, **47**, 6275-6277; (d) Z. Guo, S. Nam, S. Park and J. Yoon, *Chem. Sci.,* 2012, **3**, 2760; (e) H. S. Jung, J. H. Han, T. Pradhan, S. Kim, S. W. Lee, J. L. Sessler, T. W. Kim, C. Kang and J. S. Kim, *Biomaterials,* 2012, **33**, 945-953; (f) X. Zhou, X. Jin, G. Sun and X. Wu, *Chem. Eur. J.,* 2013, **19**, 7817-7824.

Organic & Biomolecular Chemistry Accepted Manuscript

12. X. Yang, Y. Guo and R. M. Strongin, *Org. Biomol. Chem.,* 2012, **10**, 2739-2741.

13. (a) S. P. Wang, W. J. Deng, D. Sun, M. Yan, H. Zheng and J. G. Xu, *Org. Biomol. Chem.,* 2009, **7**, 4017-4020; (b) J. Chang, Y. Lu, S. He, C. Liu, L. Zhao and X. Zeng, *Chem. Commun.,* 2013, **49**, 6259-6261.

14. (a) N. J. Leonard and R. Y. Ning, *J. Org. Chem.,* 1966, **31**, 3928-3935; (b) G. Illuminati and L. Mandolini, *Acc. Chem. Res.,* 1981, **14**, 95-102; (c) C. Galli, G. Illuminati, L. Mandolini and P. Tamborra, *J. Am. Chem. Soc.,* 1977, **99**, 2591-2597.

15. J. Gu, U. R. Anumala, F. Lo Monte, T. Kramer, R. Heyny von Haussen, J. Holzer, V. Goetschy-Meyer, G. Mall, I. Hilger, C. Czech and B. Schmidt, *Bioorg. Med. Chem. Lett.,* 2012, **22**, 7667-7671.

16. J. Ma, G. Stoter, J. Verweij and J. H. M. Schellens, *Cancer Chemother. Pharmacol.,* 1996, **38**, 391-394.

17. (a) S. Seshadri, A. Beiser, J. Selhub, P. F. Jacques, I. H. Rosenberg, R. B. D'Agostino, P. W. F. Wilson and P. A. Wolf, *N. Engl. J. Med.,* 2002, **346**, 476-483; (b) M. H. Refsum, M. P. M. Ueland, M. O. Nygård and M. D. D. P. H. S. E. Vollset, *Annu. Rev. Med.,* 1998, **49**, 31-62.

18. E. Beutler and T. Gelbart, *J. Lab. Clin. Med.,* 1985, **105**, 581-584.

19. O. Rusin, N. N. St. Luce, R. A. Agbaria, J. O. Escobedo, S. Jiang, I. M. Warner, F. B. Dawan, K. Lian and R. M. Strongin, *J. Am. Chem. Soc.,* 2003, **126**, 438-439.

20. (a) C. Lee, W. Yang and R. G. Parr, *Phys Rev B,* 1988, **37**, 785-789; (b) A. D. Becke, *J. Chem. Phys.,* 1993, **98**, 5648.

21. (a) P. J. Hay and W. R. Wadt, *J. Chem. Phys.,* 1985, **82**, 270; (b) P. J. Hay and W. R. Wadt, *J. Chem. Phys.,* 1985, **82**, 299.

Organic & Biomolecular Chemistry Accepted Manuscript

Table of contents entry
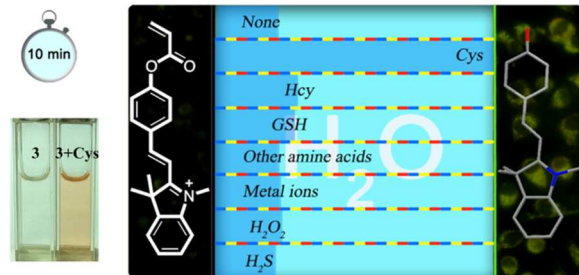
A highly selective clorimetric and ratiometric fluorescent probe for Cys was described. Furthermore, the probe could significantly distinguish Cys from Hcy and GSH by the kinetic profiles in water and diluted deproteinized human serum.